Beam Physics Note
TRI-BN-20-05
April 20, 2020

Nonlinear RF Cavities

Olivier Shelbaya

TRIUMF

Abstract: Operation of variable output energy accelerating and bunching cavities at TRIUMF-ISAC requires operator tuning of the on-axis accelerating voltage and the phase of the RF electric field. In this note, the physics of two types of accelerating RF cavity electric fields are investigated: two-gap quarter wavelength resonators as in the ISAC superconducting RF linac (SCRF), and two different interdigital H-mode (IH) accelerating tanks of the ISAC Drift Tube Linac (DTL). An analysis of the longitudinal dynamics reveals a few useful relations for variable output energy operation.

4004 Wesbrook Mall, Vancouver, B.C. Canada V6T 2A3 Tel: 604 222-1047 www.triumf.ca

1 Foreword

I write this note following discussions held over lunch with colleagues from the beam physics group. As I've both experienced accelerator physics wearing the shoes of an operator and now a physicist, I see that the use of language and jargon can sometimes lead to ambiguities or confusion, depending on prior perspective. I have also found that the formalism around the operation of RF cavities may be skewed toward a few foundational RF cavity types, while ignoring others.

To the point: the well known metric that is the transit-time factor (TTF), introduced in many texts including Wangler [1] and developed over the example of an idealized gap with a square-profile longitudinal electric field. While acknowledged as a pedagogical tool, an unhelpful feature it has at TRIUMF is that it seems to apply exactly to some RF cavities and not at all to others.

As an example, the tuning of ISAC-II superconducting linac cavities (SCB,SCC) has been carried out for over a decade now using a cosine-fitting routine on the scaled time-of-flight profile at various phases. For any cavity amplitude, operators record the time of flight (TOF) at five arbitrary phases, and from that the optimum accelerating phase is identified. There is now a `Matlab` application that performs this computation for operators, and an HLA is under development for this, as well.

On the other hand, the tuning of the ISAC-DTL is a notorious exercise for operators, particularly when it comes to the ramping or changing of its output energy. Unlike the SCRF, the majority of voltage and phase settings of the DTL tanks produce no observable beam, owing to a broadening of the energy spread which makes it vanish at the diagnostic station. As such, ISAC operators know well, and tuning procedures render explicit the need to increase the voltage and vary the phase following a very specific sequence while performing energy changes. As this is done, the energy varies in (from the operator's perspective) an unpredictable way. Finally, the TTF assuming tuning algorithm that works so well for the SCRF doesn't apply for the ISAC-DTL. You can't just fit a cosine to a DTL accelerating tank TOF or energy profile [2].

Accelerator jargon can also be ambiguous. Operators, physicists and the literature generally refer to SCRF as an accelerator and its cavities accelerating cavities, though in [3], the SCRF is referred to as 'an energy booster', implying that its cavities 'boost', but what does that mean really? Where is the line between 'boosting' and 'accelerating'? Does this have something to do with anything mentioned in this section so far? Why is the DTL hard to tune?

2 Effective vs. Scaling Voltage

Accelerating (boosting?) cavities have two basic tuneable parameters, as employed at TRIUMF-ISAC and in most, but not all, linac tuning scenarios: voltage and phase. All other cavity parameters are held constant during operation. The voltage of an axially symmetric accelerating electric field [4] is defined as:

$$V(s) = V_s \mathcal{E}(s) \tag{1}$$

where V_s is a voltage scaling factor and $\mathcal{E}(s)$ is the normalized longitudinal intensity of the electric field, whose values are by definition bound between [-1:1]. A charged particle travelling along s, the axis of symmetry of this field will experience an effective voltage which will depend on time, V_s, ϕ_0 and implicitly the particle's velocity:

$$V_{\mathit{eff}}(V_s, \phi_0, t(s)) = V_s \int_0^L \mathcal{E}(s) \cos(\omega t(s) + \phi_0) ds \tag{2}$$

An operator tuning the machine really controls the scaling voltage factor V_s through the power delivered to the cavity by the RF amplifiers. Energy change procedures call for the variation of V_s, while monitoring V_{eff} on some beam diagnostic monitor. Note that energy depends explicitly on V_s while the dependency is implicit for time:

$$\frac{dt(s)}{ds} = \frac{1}{\beta(s)c} \tag{3}$$

The problem can be summed up as follows:

$$t(s) \propto \int \frac{ds}{\beta(s)}, \qquad \beta(s) \propto \sqrt{V_{\mathit{eff}}(s)}, \qquad V_{\mathit{eff}} \propto V_s \int \mathcal{E}(s) \cos(t(s)) ds, \cdots \tag{4}$$

Now, the issue is that we really want to find the relationship $V_{\mathit{eff}}(V_s, \phi_0)$, which will allow us to understand how the operational tuning parameters affect the beam energy. I first turned my attention to the behavior of eq. (2), specifically looking at $V_{\mathit{eff}}(V_s)$ for a fixed ϕ_0. The `TRANSOPTR` model of the linac now offers a powerful platform for the numerical analysis of (4) on a variety of accelerating cavities, performed in this note.

All axially symmetric [4] electric fields $\mathcal{E}(s)$ discussed from here on are shown in figure 1: an SCB-type 2-gap quarter wave resonator, DTL Tank-1, an IH accelerating cavity with 9 gaps and DTL Tank-3, a 15 gap IH cavity. I produced the latter two on `opera-2D` using DTL technical drawings. The SCB field was provided by V. Zvyagintsev and R. Laxdal. A plot of V_{eff} and V_s, using beam input conditions corresponding to the typical operating range of the cavities, is shown in fig. 2, with an arbitrary ϕ_0 which is held constant.

Note the relative linearity of $\Delta V_{\mathit{eff}} / \Delta V_s$ for the SCB resonator compared to the IH-cavities. These curves provide insight into the behavior of the eqs. (2) and (3), notably showing the linear response of $V_{\mathit{eff}}(V_s)$ for the SCB resonator. Interestingly, both IH cavities show a strongly nonlinear response in the rate of effective voltage gain at constant ϕ_0.

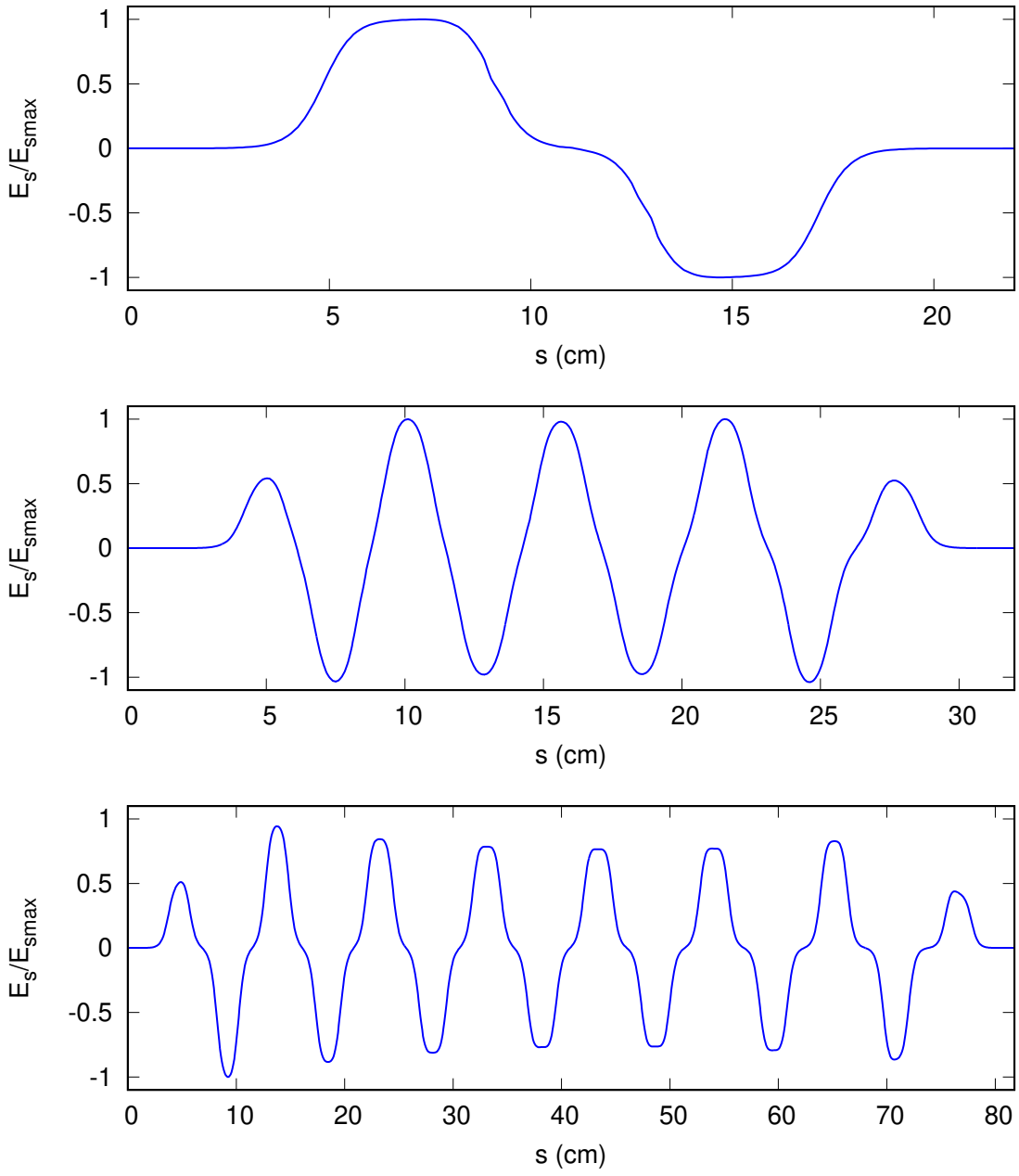

Figure 1: Longitudinal electric field distributions $\mathcal{E}(s)$ for the SCB type resonator (**top**), IH-DTL Tank1 (**middle**) and IH-DTL Tank3 (**bottom**). These were used in `TRANSOPTR` with subroutine `linac` to generate all data in the present note.

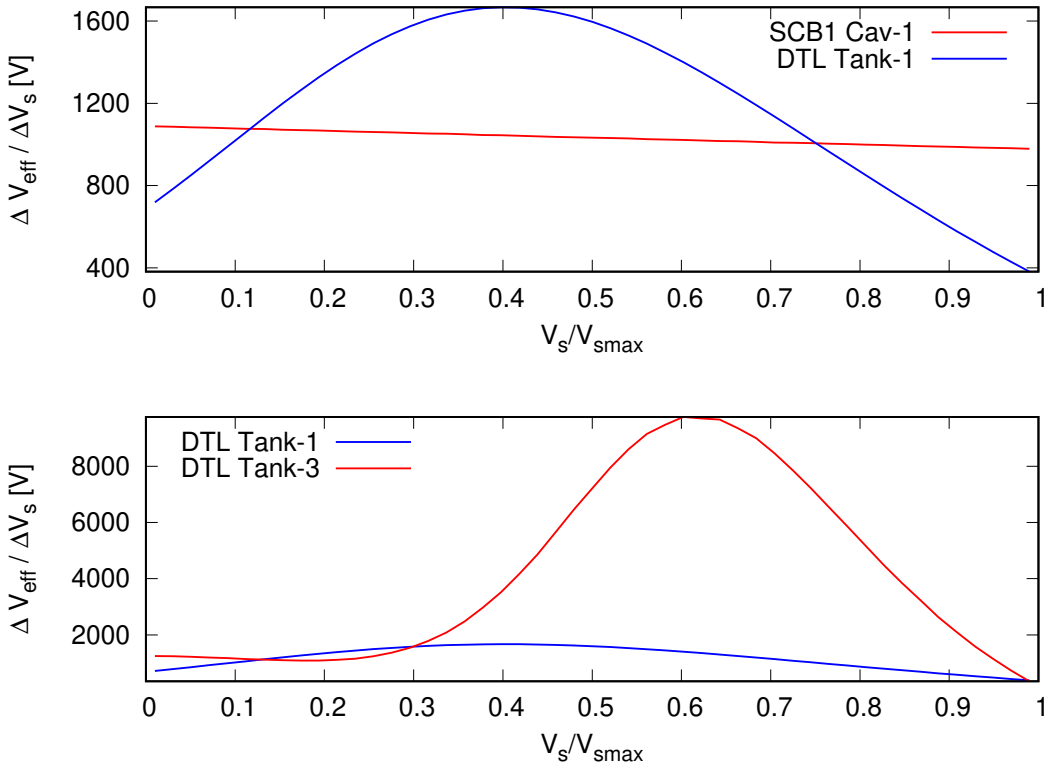

Figure 2: Comparison of the change in $V_{eff}(V_s)$ at constant ϕ_0 between an SCB-1 type resonator and DTL-Tank1 (**Top**) and between DTL-Tank1 and Tank3 (**Bottom**), both run on `TRANSOPTR`. The x-axis is the optr-voltage scaling factor used in the call to subroutine `linac`.

Turning my attention to the implicit effect of V_s on eq. (3), the optr-coordinate ct was recorded at the end of each simulation for differing values of the on-axis voltage scaling factor V_s. The total accumulated ct at the end of the simulation for each cavity was used to compute the quantity $\Delta ct/\Delta V_s$, shown in figure 3, representing the change in accumulated time at constant ϕ_0 for varying V_s. We observe that for the SCB1 resonator's case, the change in ct is approximately constant and linear to a change in V_s, especially when compared to the DTL tanks, where the change in residence time is nonlinear to ΔV_s. Since for the two-gap resonator we see a linear response in both of the cavity residence time and effective voltage to V_s, operationally one can use for the SCB resonator:

$$V_{eff} \approx kV_s \tag{5}$$

$$\Delta E \approx qkV_s \cos\phi_0 \tag{6}$$

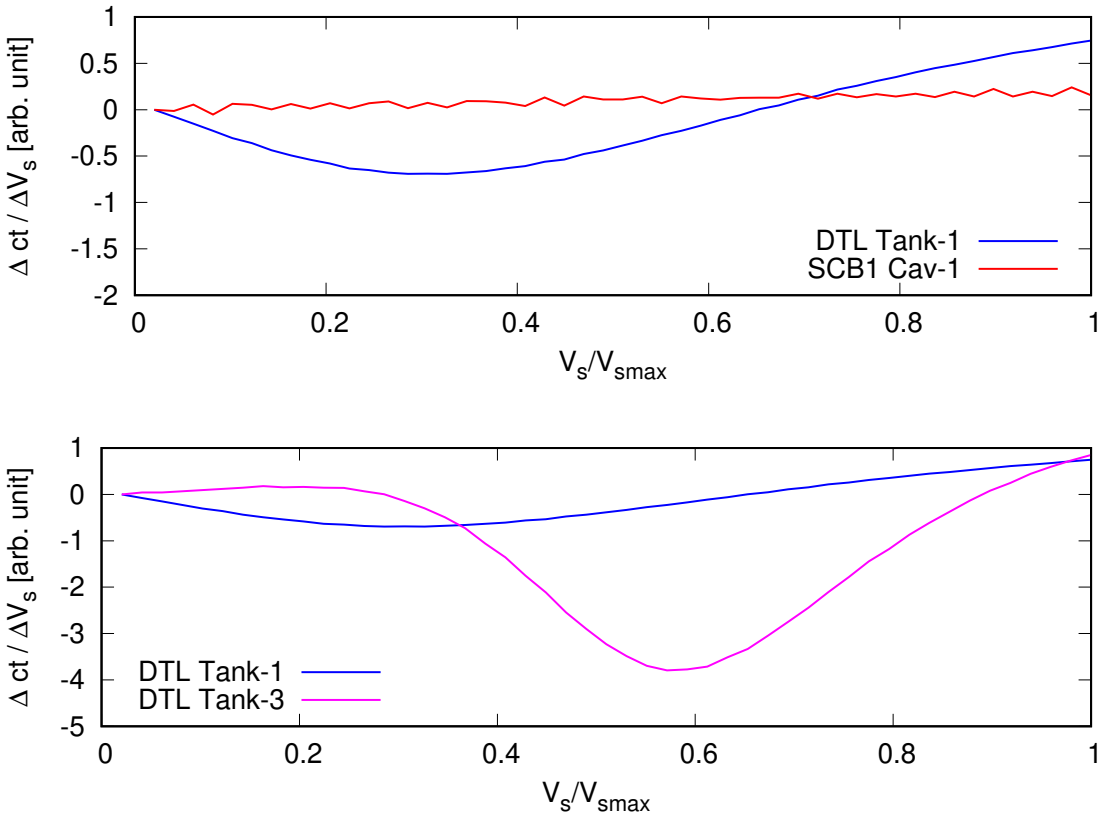

Figure 3: Computed $\Delta ct/\Delta V_s$ for (**Top**) DTL Tank-1 and SCB1-Cav1 and (**Bottom**) DTL Tank-1 and DTL Tank-3. Computations performed in `python` using `TRANSOPTR` simulation outputs. Note: the SCRF resonator produces a smaller relative energy gain, both due to the higher input energy and smaller impulse, which makes the normalization to the initial value appear to amplify the variation when compared to DTL Tank-1.

In other words, the operational tuning parameter V_s agrees almost exactly with the effective voltage on the beam, to within some linear slope that can be measured, as done for SCRF. The TOF phasing algorithm [5] assumes a perfectly sinusoidal TOF profile at the beam flight time monitors, only possible if $V_{eff}(V_s)$ is linear. The two-gap resonators can in theory display nonlinearity in $V_{eff}(V_s)$, however for this it is necessary to considerably increase V_s. This is shown in figure 4, where the resonator was run with up to 10 times the maximum allowable V_s. In practice, this far exceeds what can either be produced or safely handled by the amplifiers or RF cavity. And so, in daily operation, the SCB resonator's tuning voltage agrees well enough with the effective voltage, that eq. (6) can be used.

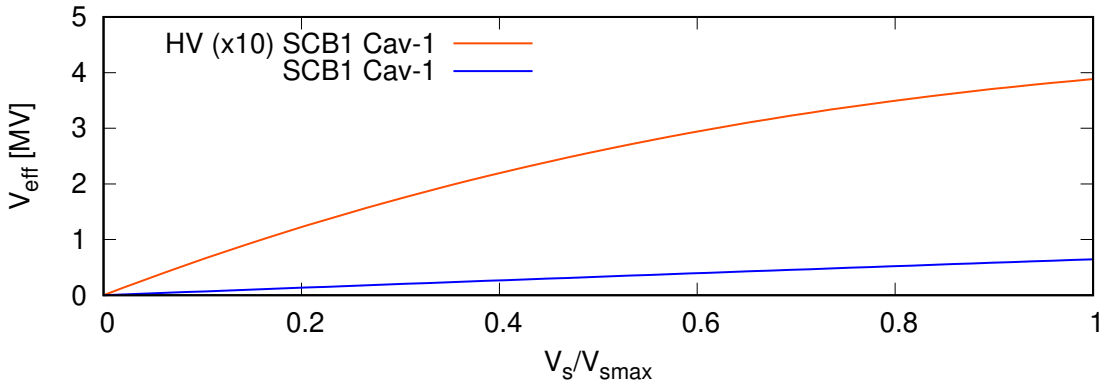

Figure 4: Comparison of $V_{eff}(V_s)$ for the same SCB-1 type resonator on its operational range of V_s (**blue**) and with ten times more V_s scaling that operationally allowable (**red**), showing emergent nonlinearities in the effective voltage. The x-axis is the optr-voltage scaling factor used in the call to subroutine `linac`.

3 From a Factor to a Landscape

For the case of the IH DTL tanks, since the relationship between both V_{eff} and cavity residence time is nonlinear, we cannot use eq. (6), as the cavity output depends on both (V_s, ϕ_0). And so, instead of seeking to relate V_{eff} to V_s using a constant, we are constrained to evaluate a factor which is a two dimensional function of both tuning parameters:

$$V_{eff} = V_s \mathcal{T}(V_s, \phi_0) \tag{7}$$

where:

$$\mathcal{T}(V_s, \phi_0) = \int_0^L \mathcal{E}(s) \cos(\omega t(s) + \phi_0) ds \tag{8}$$

With the caveat that the quantity $\mathcal{T}(V_s, \phi_0)$ is a gain parameter which appropriately couples the on-axis voltage scaling parameter V_s and the effective voltage. It is the landscape of transit efficiencies in cavity tuning parameter configuration space. It is clear that this is analogous to the numerator of the transit time factor (TTF):

$$T = \frac{\int_{-L/2}^{L/2} E(0,z) \cos(2\pi z/\beta\lambda) dz}{\int_{-L/2}^{L/2} E(0,z) dz} \tag{9}$$

and the denominator is the height of the square field voltage [1]. Also note that in eq. (7), $\mathcal{E}(s)$ is already normalized to its maximum, echoing Wangler's definition. Should we wish to use the square gap TTF (9) for a variable energy IH cavity, we would be constrained to compute it for each (V_s, ϕ_0) pair due to the nonlinearity between effective voltage and scaling factor: the definition has lost its advantage. We must evaluate $\mathcal{T}(V_s, \phi_0)$ of eq. (7).

In relation to my initial questioning, I advance that it is not unreasonable to use the behavior of $V_{\mathit{eff}}(V_s)$ to draw the line at what defines a 'Booster' and an 'Accelerator' cavity: is the relationship linear across the range of operable V_s, or not? Regardless, this is a matter of jargon and convention. All this is really just notational window dressing for what is the fundamental statement:

$$E(V_s, \phi_0) = E_0 + qV_s \int_0^L \mathcal{E}(s) \cos(\omega t(s) + \phi_0) ds \tag{10}$$

To be sure, I used `topology` to generate surveys of $V_{\mathit{eff}}(V_s, \phi_0)$ and see. Using the `TRANSOPTR` model of the linac, I ran simulations for each case iterating (V_s, ϕ_0) from $(0, V_{smax})$ and $(0°, 360°)$, with maximum V_s values taken from [6] for the DTL and from the operational calibrations for SCB. The projection of the set of all values of $V_{\mathit{eff}}(V_s, \phi_0)$ on a surface normal to the ϕ_0 and V_{eff} axes shows the (non) linearity for each cavity.

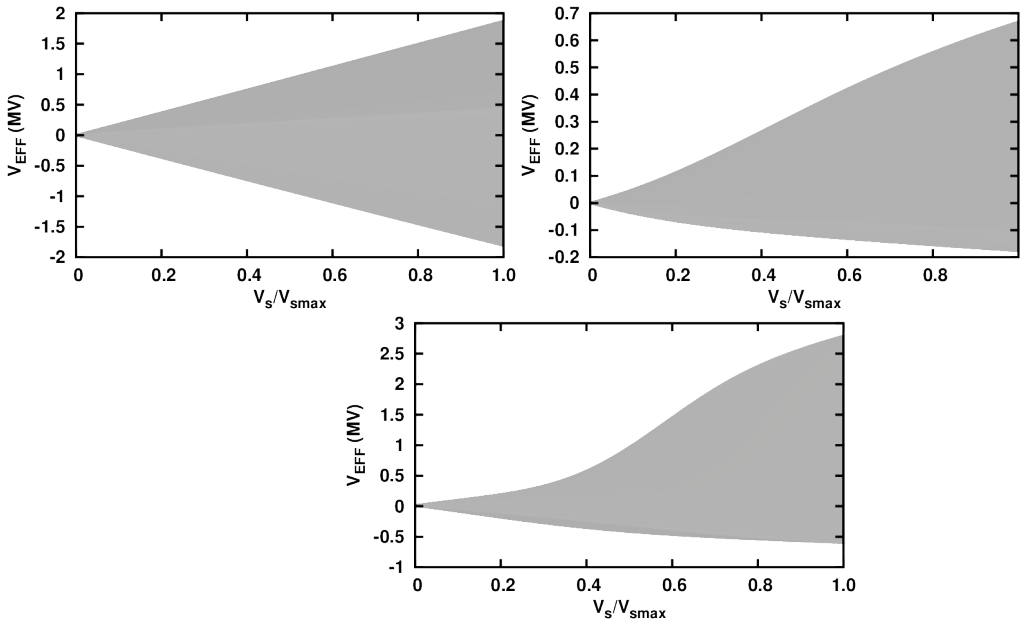

Figure 5: Projection of $V_{\mathit{eff}}(V_s, \phi_0)$, showing the envelope of $V_{\mathit{eff}}(V_s)$ for all ϕ_0. Cases shown are (**Top-L:**) an SCB-1 type resonator. (**Top-R:**) DTL Tank-1. (**Bottom:**) DTL Tank-3. Simulated in `TRANSOPTR`.

The accelerating profile of the IH DTL tanks introduces strong nonlinearities in the effective voltage's response to a linear ramping of V_s, for any phase. Because the tanks feature an accelerating gradient, in other words a varying longitudinal peak-to-peak spacing in $\mathcal{E}(s)$ and since they feature more gaps, the solution space for the reference trajectory at any given (V_s, ϕ_0) grows, shown for DTL Tank-1 in figure 6.

For certain initial conditions in the multigap cavity, the acceleration may abruptly reverse course while incrementing V_s, unlike for a two gap resonator. Each of the shown $d\beta/ds$ curves in fig. 6 are produced at the same cavity ϕ_0, but for different voltage scaling. The corresponding energy profile is shown at the bottom. It is worth noting that the curve labeled 'V_s 3' corresponds to the highest V_s value of all three cases shown.

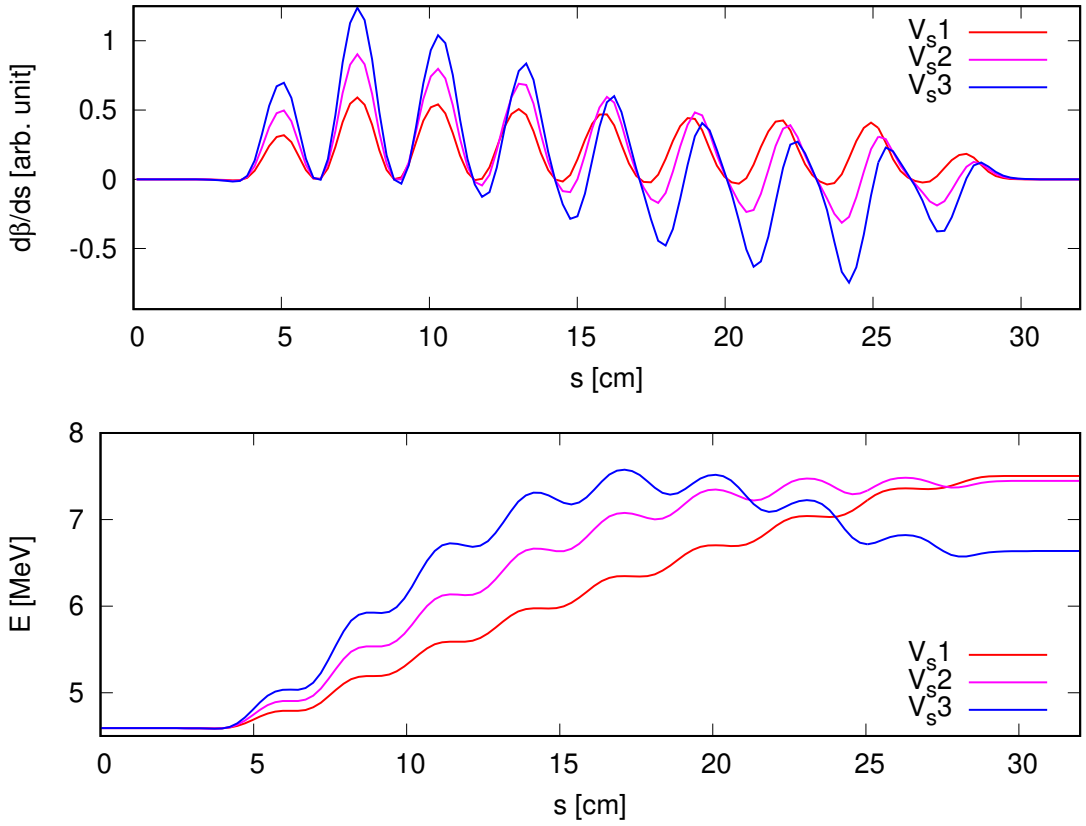

Figure 6: Reference particle $d\beta/ds$ (**Top**) and energy (**Bottom**) through DTL Tank-1 for three scaling factor voltages, V_s 1 to 3, with $V_s1 < V_s2 < V_s3$. The RF cavity phase ϕ_0 is identical for each case.

4 The Debunching Effective Voltage

Consider a bunch arriving at an accelerating field $\mathcal{E}(s)$ at a time t_0 with a centroid E_0. A high energy front and low energy tail which deviate from the bunch centroid by $\pm\Delta E_0$ define the particle distribution in longitudinal configuration space. And so, the first particles enter the field at a time $t_0 - \Delta t$ and we require $\omega\Delta t \ll 2\pi$. The output energy for the former is the charge q times the effective voltage of eq. (2):

$$E_f = E_0 + \Delta E_F + qV_{eff}\sin(\phi_0 - \omega\Delta t) \tag{11}$$

$$E_f = E_0 + \Delta E_F + qV_{eff}\sin\phi_0 - qV_{eff}(\omega\Delta t)\cos\phi_0 \tag{12}$$

In order to preserve bunch coherence up to the target, we want the energy spread ΔE_F at the output to be minimized, thereby reducing longitudinal bunch growth. This is also known as the debunching voltage. Consider the case where the energy spread and $\omega\Delta t$ contribution cancel at a given phase:

$$\Delta E_F = qV_{eff}\omega\Delta t\cos\phi_0 \tag{13}$$

Though ΔE_F is constant and the $\omega\Delta t$ term is oscillatory in ϕ_0. The difference can be minimized at any ϕ_0 by choosing to set:

$$V_{eff} = \frac{V_0}{\cos\phi_0} \tag{14}$$

V_0 is the debunching effective voltage, at a measured point (V_{s0}, ϕ_0), for which the output energy remains unchanged and the phase ϕ_0 is referenced to this point. Setting the effective voltage to (14) will minimize the bunch energy spread to:

$$\Delta E_F - qV_0\omega\Delta t \tag{15}$$

which in turn allows for a minimization of the longitudinal divergence. In other words, by setting V_s = $V_{s0}/\cos(\phi_0 - \phi)$, one obtains optimum debunching at variable output energy. This relationship is of significant interest to variable energy two-gap cavity operation. The full output energy spectrum of the three discussed cases are shown in figure 7. The sinusoidal effective voltage profile can be seen for the SCB resonator: any line of constant V_s will feature a full sinusoidal oscillation in V_{eff} over 360°. However, for both IH tanks this is clearly not the case. Though cyclical over 360°, equation 2 produces a highly nonsinusoidal effective voltage at constant V_s.

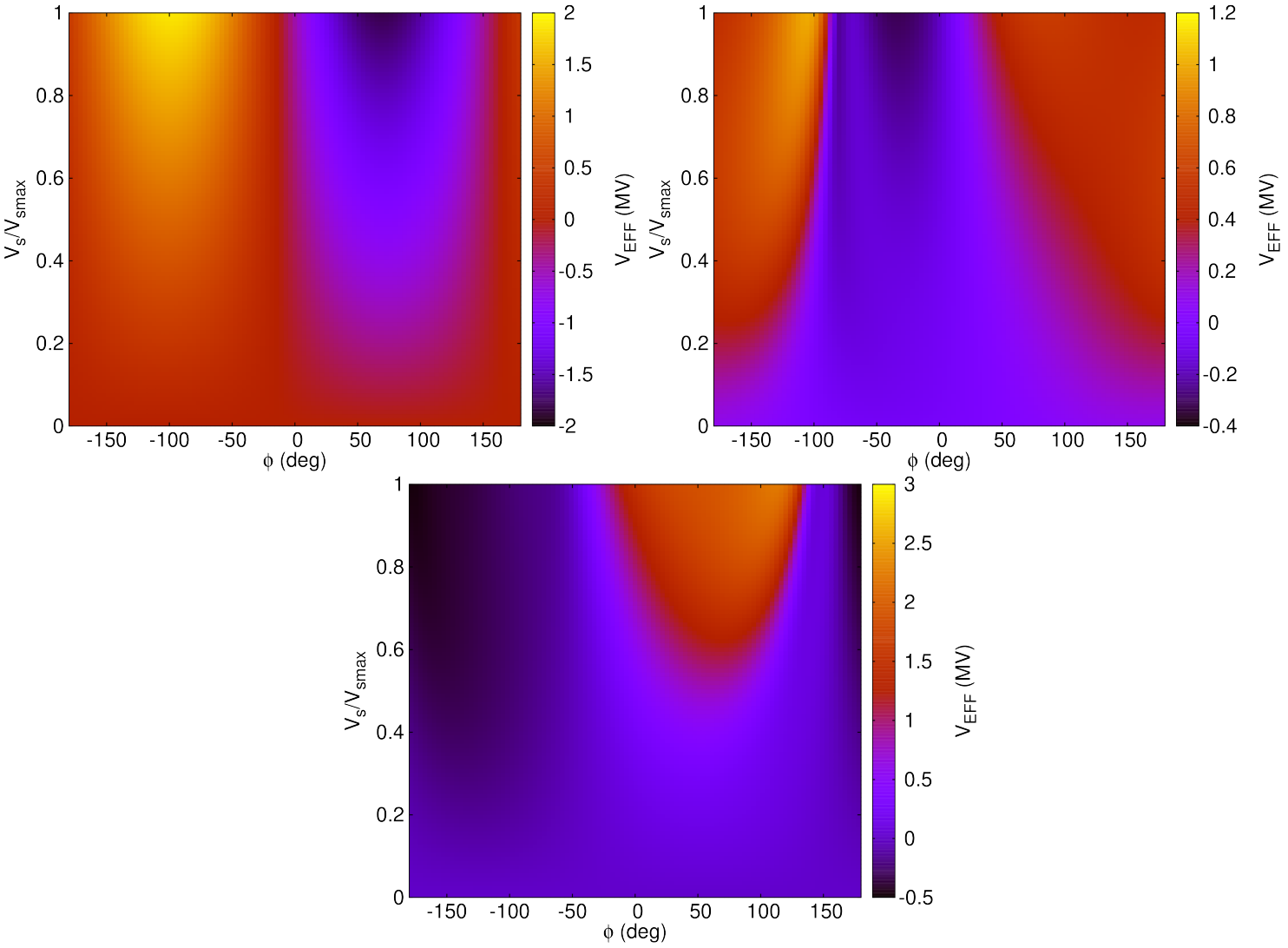

Figure 7: **Left:** TRANSOPTR effective voltage, as measured at the corresponding downstream energy diagnostic station: HEBT1:MB0 for the DTL and SEBT:FTM20 for SCB.(**Top-L:**) SCB1 resonator , (**Top-R:**) DTL Tank1, (**Bottom:**) DTL Tank3. All scans defined on a 100 by 100 grid.

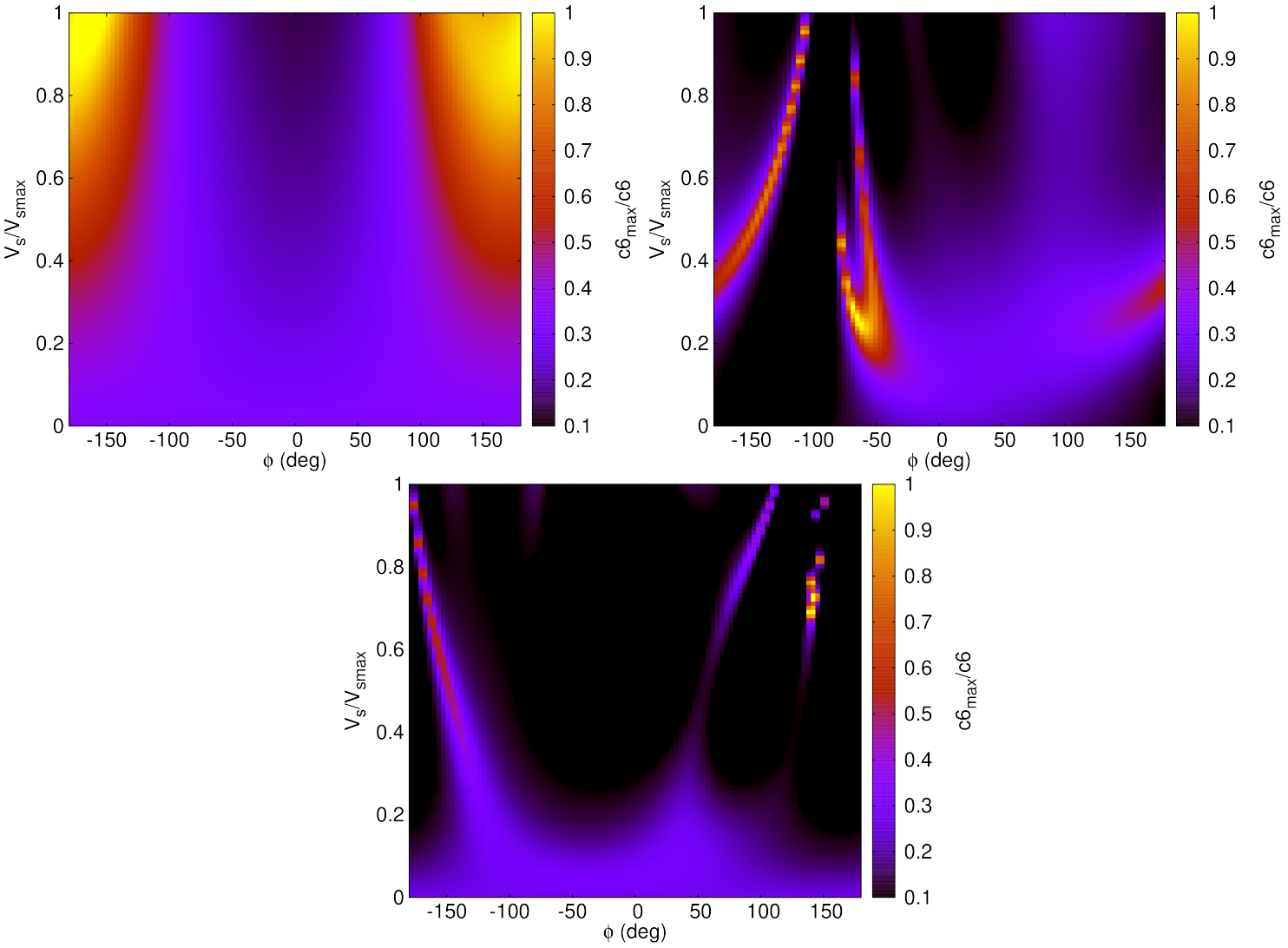

Figure 8: **Left:** `TRANSOPTR` relative normalized inverse bunch momentum, as measured at the corresponding downstream energy diagnostic station: HEBT1:MB0 for the DTL and SEBT:FTM20 for SCB.(**Top-L:**) SCB1 resonator , (**Top-R:**) DTL Tank1, (**Bottom:**) DTL Tank3. All scans defined on a 100 by 100 grid.

In fig. 8, the inverse of TRANSOPTR coordinate P_z is plotted, being the longitudinal bunch momentum in the co-moving reference particle frame along s. Each dataset has been normalized to the maximum. Since P_z = $\Delta E/\beta c$, the inverse momentum is a quantity which is large when the energy spread is minimized. The figure has purposely been cut off at 10% relative to the maximum and all values shown are recorded at either downstream diagnostic station: the Prague for the DTL cases and SEBT:FTM20 for the SCB case.

The colorscale cutoff in fig. 8 is chosen to represent loss of observable beam. If the energy spread grows too much, the energy distribution or TOF spectrum will not be measurable on either diagnostic. The value of 10% was chosen as an example and not an exact representation of detector ranges. Nevertheless, we do observe that for the DTL tanks, a vast swath of (V_s, ϕ_0) configuration space produces unobservable beam.

For SCB, while the beam quality can be made sufficiently bad as to be unobservable, we note that this region is smaller and features a clearly defined boundary: equation 14. The linearity of $V_{eff}(V_s)$ also means operators can always expect a relatively predictable sinusoidal like energy variation any time they move ϕ_0, unlike the DTL. Its strong nonlinear response means that a given V_s input will have a vastly different effect on the output energy at different phases. This also visibly deforms the region of optimal debunching in (V_s, ϕ_0).

The solutions with minimum energy spread are also much narrower for the nonlinear cavities: when one establishes a such a condition, a small phase change can cause a sharp change in output beam properties, including longitudinal bunch growth, but more importantly loss of transmission due to changed beam energy. Figure 6 shows why: many of the output energy configurations subject the bunch to considerable acceleration and restoring forces - an inefficient path to an intermediate output energy. The minimization of the output energy spread is really a sign that the path of least resistance has been taken. This renders clear why ramping DTL tanks in energy while continually monitoring beam on a diagnostic requires following a very specific path in (V_s, ϕ_0) space. Incidentally, the script `pathfinder` [7] coupled with `topology` can extract this optimum $V_s(\phi)$ parametrization for each of the above tanks, giving us an ability to keep the phase constantly optimized for any input V_s.

As a closing thought, this is really just a consequence of the IH cavities having so many gaps all tied to the same phase and voltage. Unlike a long sequence of independently controlled two-gap boosters, in an accelerating tank, the more gaps there are, the more constrained the bunch is to follow the synchronous profile of the reference particle. I now have an answer to my initial question of why the DTL is so hard to tune.

Acknowledgements

Many thanks to Rick Baartman, Thomas Planche and Paul Jung for the many lunchtime discussions on this topic. Tiffany Angus, Spencer Kiy and Marco Marchetto are also thanked, each who helped train me on operational tuning. Rick Baartman also helped me navigate the debunching example concept, on top of patiently answering my many questions and providing feedback.

References

[1] T.P. Wangler. *RF Linear Accelerators, 2nd Edition*. Wiley-VCH, 2008.

[2] M Marchetto, J Berring, and RE Laxdal. Upgrade of the isac dtl tuning procedure at triumf. *EPAC08, Genoa*, page 3440, 2008.

[3] RE Laxdal, W Andersson, K Fong, M Marchetto, AK Mitra, WR Rawnsley, and I Sekachev. Commissioning of the isac-ii superconducting linac at triumf. In *Proc. Of EPAC*, 2006.

[4] R. Baartman. Linac Envelope Optics. Technical Report TRI-BN-15-03, TRIUMF, 2015.

[5] Spencer Kiy, Olivier Shelbaya, Marco Marchetto, Robert Laxdal, and Stephanie Rädel. Beam-based measurements of the isac-ii superconducting heavy ion linac. In *Proceedings of the 9th International Particle Accelerator Conference*, pages 4832–35, 2018.

[6] AK Mitra, PJ Bricault, IV Bylinskii, K Fong, G Dutto, RE Laxdal, RL Poirier, et al. *RF Test and Commissioning of the Radio Frequency Structures of the TRIUMF ISAC I facility*. In *Proceedings of LINAC*, page 106, 2002.

[7] O. Shelbaya. Longitudinal Beam Topology with TRANSOPTR. Technical Report TRI-BN-20-01, TRIUMF, 2020.